ADVANCED MATERIALS INTERFACES
www.advmatinterfaces.de

Plasma-Assisted Surface Modification and Heparin Immobilization: Dual-Functionalized Blood-Contacting Biomaterials with Improved Hemocompatibility and Antibacterial Features

Hatice Ferda Özgüzar, Ebru Evren, Ahmet Ersin Meydan, Gozde Kabay, Julide Sedef Göçmen, Fatih Buyukserin, and Osman Erogul*

The inferior hemocompatibility or antibacterial properties of blood-contacting materials and devices are restraining factors that hinder their successful clinical utilization. To highlight these, a plasma-enhanced modification strategy is favored for surface tailoring of an extensively used biomaterial, polypropylene (PP). The surface activation of the PPs is achieved by oxygen plasma etching and subsequent surface functionalization through amine-rich precursor mediated coating by plasma glow discharge. After optimum plasma processing parameters are decided, heparin (anticoagulant and antithrombic drug) is either attached or covalently conjugated on the PPs' surfaces. The aminated films produced at 75 W plasma power with 15 min exposure time are highly hydrophilic (34.72 ± 5.92°) and surface active (65.91 mJ m^{-2}), facilitating high capacity heparin immobilization (≈440 µg cm^{-2}) by covalent linkage. The kinetic-blood coagulation rate and protein adhesion amount on the plasma-mediated heparinized PPs are decreased about tenfold and 15-fold, and platelet adhesion is markedly lowered. In addition, heparinized-PP surfaces comprise superior antibacterial activity against gram-positive/-negative bacteria conveyed particularly by contact-killing (99%). The heparin-coating did not cause cytotoxicity on fibroblast cells, instead enhanced their proliferation, as shown by the (3-(4,5-Dimethylthiazol-2-yl)-2,5-Diphenyltetrazolium Bromide) assay. Overall, this simple methodology is highly proficient in becoming a universal strategy for developing dual-functionalized blood-contacting materials.

1. Introduction

Foreign body reaction refers to the exerted immune response against the implanted material that converges multiple reactive mechanisms, including platelets, coagulation cascade, and complement system activation, protein adsorption, and bacteria accumulation.[1–5] Despite an efficient host immune system, such mechanisms can lead to thrombogenesis and infection persistence in the long term. So far, numerous substrate materials and surface coating strategies have been investigated to overcome these pitfalls and improve the implanted biomaterials' blood compatibility and antibacterial performance.[6–10]

For instance, owing to remarkable physicochemical properties such as high strength, low cost, lightweight, high thermal and chemical stability, ease of processing, and long flex life, polypropylene (PP) material plays a vital role in a wide application area ranging from clinical apparatus and cardiovascular implants to medical devices development.[11]

H. F. Özgüzar, A. E. Meydan, G. Kabay
Plasma Aided Biomedical Research Group (pabmed)
Biomedical Engineering Division
Graduate School of Engineering and Science
TOBB University of Economics and Technology
Ankara 06560, Turkey
E-mail: hfozguzar@etu.edu.tr

H. F. Özgüzar
Department of Materials Engineering
Biomaterials and Tissue Engineering Research Group
KU Leuven
Leuven 3000, Belgium

The ORCID identification number(s) for the author(s) of this article can be found under https://doi.org/10.1002/admi.202202009.

DOI: 10.1002/admi.202202009

E. Evren
Department of Medical Microbiology
Ankara University School of Medicine
Ankara 06620, Turkey

A. E. Meydan, J. S. Göçmen
Department of Medical Microbiology
Faculty of Medicine
TOBB University of Economics and Technology
Ankara 06560, Turkey

G. Kabay
Karlsruhe Institute of Technology
Institute of Functional Interfaces (IFG)
76344, Karlsruhe, Germany

F. Buyukserin, O. Erogul
Department of Biomedical Engineering
Faculty of Engineering
TOBB University of Economics and Technology
Ankara 06560, Turkey

Nevertheless, the major hurdles in using PP as a biomaterial are its long-term thrombogenicity and poor host tissue adhesiveness, possibly due to inherent surface properties (low surface energy and lack of polar functional groups) and poor blood compatibility.[12] Hence, significant research has been conducted to improve the surface features and biocompatibility of PP.

Immobilizing biomolecules on polymer surfaces proved to be an effective strategy to improve the host tissue adhesion and biocompatibility features of the substrate material of interest. Up to date, several biomolecules, such as insulin,[13] gelatin,[14] collagen,[15] chitosan,[16] lysine,[17,18] and heparin,[4,9,7,12,16–26] have been immobilized on various polymer surfaces. Heparin stands out due to its capability to bind to and enhance the inhibitory activity of the plasma protein antithrombin against several serine proteases of the coagulation system, most importantly factors IIa (thrombin), Xa, and IXa. Although it has been extensively used in clinics (particularly in pre- and post-operation stages of blood-contacting materials surgery), several complications, including bleeding, bruising, and thrombocytopenia, limit its long-term usage.[27] To eliminate such downsides while retaining the anticoagulant activity of the free-heparin, various conjugation methods through attachment or chemical bonding onto material surfaces have been utilized, particularly after performing plasma activation and functionalization of the non-woven PP fabrics or via photografting technology.[28,29] For instance, PP surfaces were modified by photo-grafting hydroxyethyl acrylate and vinyltriethoxysilicane under UV light irradiation for heparin immobilization. Although heparin's presence halved the hemolysis ratio compared with unmodified PP substrates, a detailed investigation of antibacterial features and other hemocompatibility indicators has not been carried out.[30] In another study, PP surfaces were activated with a cold atmospheric plasma polymerization method to facilitate subsequent grafting of acrylic acid and polyethylene glycol. Following that, not only heparin but also chitosan and insulin were bound to the modified PP surfaces that yielded an increased hemocompatibility (decreased adhesion and activation of platelets and adsorption of plasma proteins) compared to unmodified PP.[12] Alternatively, another group utilized PP surface activation accompanied by Argon plasma etching and plasma polymerization mediated film formation by acrylic acid grafting to immobilize the heparin and gentamicin solely or as a biocomplex. Although both anticoagulant (with hemolysis test) and antibacterial features (against *S. aureus*) of the functionalized material were improved, the developed strategy is only suitable when the PPs were intended to be used as a non-woven therapeutic textile material.[19]

As reviewed above, most studies focused on PP substrates as non-woven fabrics and evaluated their features within that perspective. In this study, however, we introduced heparin immobilized PPs as a blood-contacting material and investigated its features by conducting serial chemical and physical analyses and through an extensive biological evaluation according to the assured criteria.[31] In addition, although heparin has been in clinical use for a long time, its antimicrobial effect and mechanism are not well investigated. Therefore, this study revealed the antibacterial mechanism of heparin against three bacteria strains, gram-negative *E. coli*, gram-positive *S. aureus,* and *S. epidermidis*. In hemolysis and platelet adhesion studies, heparin's anticoagulant activity was investigated further on bare and heparin immobilized PPs.

2. Experimental Section

2.1. Materials

Heparin sodium salt (Grade I-A, ≥180 USP units mg^{-1}), *N*-(3-dimethyl aminopropyl)-*N*'-ethyl carbodiimide (EDC), *N*-hydroxysuccinimide (NHS), toluidine blue dye, citrate buffer solution (0.09 M), bovine serum albumin (BSA), glutaraldehyde (25% in H_2O) polypropylene sheets (10 m length × 0.05 mm depth), minimum essential medium (MEM), fetal bovine serum (FBS), sodium pyruvate solution, Dulbecco's phosphate buffered saline (DPBS), and 3-(4,5-dimethylthiazol-2-yl)-2,5-diphenyltetrazolium bromide (MTT) were purchased from Sigma-Aldrich (NJ, USA). L-glutamine, penicillin-streptomycin, 0.25% Trypsin, and 0.005% EDTA were acquired from Biological Industries Ltd. (Haemek, Israel). Normal human BJ skin fibroblast (ATCC CRL-2522) cell lines were supplied from American type culture collection (ATCC, VA, USA). Dimethylsulfoxide (DMSO) and ethanol was obtained from ISOLAB Laborgeräte GmbH (Eschau, Germany).

2.2. Sample Preparation and Plasma Modification

First, the polypropylene (PP) sheets were cut into 1 × 1 cm^2 pieces and cleaned with ethanol and ultra-pure water in an ultrasonic bath for 30 min. The cleaning process was replicated three times before air drying. Each piece was placed on glass slides and kept in a desiccator until further use.

A dual-step plasma modification was performed using a radio frequency/low pressure (RF/LP) (13.56 MHz) plasma device (Pico, Diener Electronic GmbH, Germany) by individually placing each substrate material in the middle of a stainless-steel chamber (150 mm radius/320 mm length). Before each plasma processing step, first, the evacuation of the plasma chambers was proceeded by a vacuum pump (Trivac 2.5E, Leybold Vacuum GmbH, Germany) until the pressure went down to 0.14 mbar. To avoid contamination, the chamber was washed (100 W discharge power for 15 min) with the same precursor (O_2 or amine-rich precursors) to be utilized at the following modification steps.[31–33]

First, surface activation of bare polypropylene (b-PPs) substrates was carried out by O_2 plasma-assisted etching at 100 W discharge power for 15 min.[31] In the second step, the O_2-activated PP substrate (O_2—PPs) surfaces were exposed to ethylenediamine (EDA) and ammonia (NH_3) precursor mixture [EDA:NH_3, 1:1 (v:v)] mediated glow discharge. To form amine-rich thin films on the O_2-activated PPs (NH_2—O_2—PPs), plasma discharge power was varied between 25 and 100 W, whereas the exposure time and pressure were kept constant at 15 min and 0.14 mbar.

2.3. Heparin Immobilization

Heparin is a heterogeneously structured polyanionic mucopolysaccharide comprising chemically reactive carboxyl (−COOH), hydroxyl (−OH), and sulfonate ($-SO_3^-$) groups. Since systematically administrated free dosage of heparin can lead to severe immunologic reactions, for example, bleeding and shortness of breath, effective immobilization of heparin to blood-contacting material is crucial and should be carefully optimized.[27]

In this study, the influence of two immobilization methods on heparin immobilization capacity and biological activity are investiagted: Electrostatic adsorption and cross-linking. Physical adsorption was achieved by directly treating substrates with varying concentrations of heparin prepared in a citrate buffer (3, 10, and 30 mg mL^{-1}, pH: 4.7). Yet, to form covalent bonding, EDC and NHS mixture [EDC:NHS, 4:1 (w:w)] were simultaneously added to heparin-containing solutions [1:1 (w:w)].[34] The mixture was stirred for 3 h at 25 °C to activate carboxyl groups on heparin, which were later chemically bound to the amino groups generated on the plasma-modified film's surface. Moreover, unmodified b-PPs, plasma-modified O_2−PPs, and NH_2−O_2−PPs were subjected to heparin solutions (hep refers to conditions for physical binding, and hep* refers to conditions of chemical bonding) and agitated in a shaking incubator (Innova 40R, New Brunswick, DE) at 37 °C for 24 h. The heparin immobilized surfaces were washed with PBS (pH:7.4) and UPW to remove excess heparin, which was simultaneously confirmed by the toluidine blue (TB) method.[35] A detailed representation of all production and biological testing stages is given in **Figure 1**.

2.4. Plasma Parameter Optimization and Characterization

For the optimization of plasma processing parameters, first, the surface topographies of PP substrates were examined under an atomic force microscope (AFM, Asylum, Asylum Research, Oxford Instruments, Oxford, UK) using a PPP-type cantilever (Nanoworld AG, Matterhorn, Switzerland) in a tapping mode. Unmodified b-PPs were taken as a reference, and measurements were replicated three times. Root mean square roughness (*Rq*) of the plasma (un)modified films were evaluated. Following that, an X-ray photoelectron spectroscopy (XPS) instrument (Thermo K-Alpha (Thermo Fisher Sci., Waltham, MA, USA) was used to characterize the elemental composition of bare and plasma-modified PPs. Randomly selected substrate portions were analyzed using an X-ray beam focused at 400 µm under 1×10^{-9} Torr pressure. The XPS spectra were recorded with an energy step width of 0.8 eV, an acquisition time of 160 ms per data point, and analyzer pass energies of 187.85 eV.

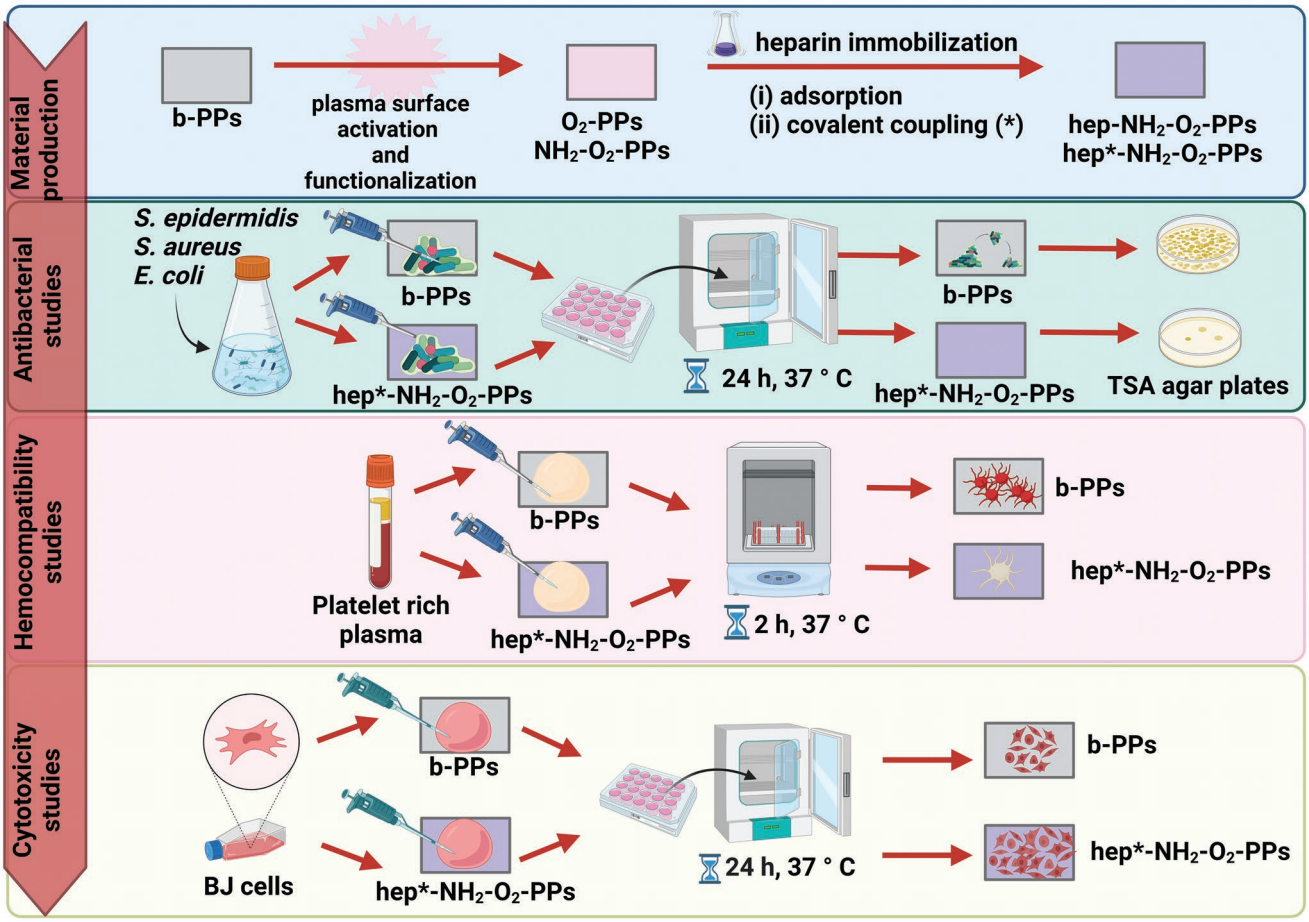

Figure 1. Schematic representation of the multiple stages performed for plasma-assisted biomaterials production and biological testing.

After deciding optimal plasma processing parameters and subsequent heparin immobilization, the functional groups formed on the b-PPs were analyzed by Fourier transform infrared spectroscopy (ATR-FTIR, Thermo Fisher Sci., Waltham, MA, USA) that was performed within the wavenumber range of 4000–1000 cm^{-1}. After that, contact angle (CA) measurements were made using the sessile drop technique to investigate the wettability features of the plasma-modified PPs and calculate their associated surface free energies (SFE) by Fowke's equation.[36,37] A contact angle analyzer (KSV Instruments Ltd., Finland) was used to examine sessile drops (10 µL) consisting of deionized water (polar) and diiodomethane (dispersive) placed on the PPs' surfaces.

A scanning electron microscope (SEM) (SEM, FEI-Quanta 400 F, TX, USA) imaging was performed to evaluate bacterial and platelet adhesion features of the heparinized PPs. The accelerating voltage and spot size were adjusted to 5–10 kV and 2.0 µm, respectively.

OriginLab v.6 (Wellesley Hills, MA, USA) was used for data evaluation, statistical calculations, and representation. The One-way ANOVA (Analysis of variance) was performed to compare the datasets and to determine the statistical significance of the selected sample groups ($*p \leq 0.05$). The results are reported as mean ± standard deviation (mean ± SD) of replicated measurements.

2.5. Immobilization Capacity and Stability

The substrates were immersed in PBS (pH:7.4) consisting of toluidine blue (TB, 2 mL of 7.5 ppm) dye to determine the surface density of both physically adsorbed and cross-linked heparin (hep−NH_2−O_2−PPs and hep*-NH_2−O_2−PPs). All samples were agitated in a shaking incubator at 50 rpm for 20 min, transferred to an ultrasonic bath for 10 min, and subsequently vortexed (1 min). The buffer medium was aliquoted and tested by UV–vis spectroscopy to screen absorbance values at 630 nm after substrate removal. Ultimately, the immobilized heparin amounts were calculated using the calibration curve, which was previously obtained for varying concentrations of free-heparin prepared in the TB solution (Figure S1, Supporting Information).

A similar procedure was followed to investigate immobilized heparin's (hep and hep*) stability on the PP surfaces. Briefly, bare, physically adsorbed, or cross-linked heparin-comprising samples were dipped into 5 mL of PBS (pH:7.4) solution and placed into a shaking incubator for continuous stirring for 30 days (37 °C, 50 rpm). The remaining surface density of the immobilized heparin hence the stability on the differently pre-modified PP substrates, was determined by testing the sampled buffer at the predetermined time points (24, 120, 360, and 720 h) at which the PP samples were taken out, washed with UPW, and dried in the vacuum oven (37 °C, 2 h).

2.6. Protein Adhesion

When a material encounters blood, the first event realized at the material surface is the adsorption of blood proteins, for example, albumin, fibrinogen, and globulin. Subsequently, adhered proteins initiate the adhesion and activation of platelets, which may lead to the formation of neighboring platelets. Finally, the thrombi are stabilized by the generation of a fibrin network at the blood-material interface. Therefore, investigating its protein adhesion features is critical after a blood-contacting material development because it plays a significant role in the living vasculature.[38,39] Hence, the protein adhesion features of the PP substrates were tested against the model protein, BSA. For the evaluation of the influence of bound-heparin on protein adhesion, unmodified and heparin-immobilized samples (hep−NH_2−O_2−PPs and hep*-NH_2−O_2−PPs) were treated with BSA solution (1 mg mL^{-1} in PBS (0.1 M, pH: 7.4)). All samples were transferred to a shaking incubator (37 °C) and continuously stirred at 50 rpm for 10 days. At predetermined time points (0, 24, 48, 120, and 240 h), 500 µL of buffer medium was collected and substituted with fresh buffer. The surface-bound protein concentration was then determined by subtracting the calculated free BSA concentration from the initial BSA concentration obtained from UV–vis spectroscopy analyses at 280 nm.

2.7. In Vitro Antibacterial Testing

It is well documented that implanted materials, such as stents and vascular grafts, are susceptible to bacterial colonization formation on their surface due to their inadequate antibacterial properties, which can result in severe inflammatory responses.[20,40,41] For example, *S. epidermidis* (*S. epidermidis,* a gram-positive and coagulase-negative bacterium) has been identified as the primary pathogen responsible for biomaterial- and hospital-related infections.[42] Therefore, in this study, the antibacterial properties of the heparinized PPs and heparin solutions were tested against three bacteria strains: Gram-positive *S. epidermidis* (ATCC 35 984, highly resistant)[43]*and S. aureus* (ATCC 25 923), and gram-negative *E. coli* (ATCC 25 922).

First, the antimicrobial properties of free heparin were studied. The optimum free heparin concentrations equivalent to minimum inhibition concentration (MIC) and minimum bactericidal concentration (MBC)[10] were calculated. Detailed information regarding the MIC and MBC determination method and the accompanying data are given in Supporting Information.

In the second stage, the antibacterial features of heparinized-PPs were analyzed to see the influence of heparin immobilization compared to its free dosage counterpart by following a previously described procedure.[44,45] Briefly, all bacteria strains were incubated in a TSB medium, and 10 µL bacteria cells (1.5×10^6 CFU mL^{-1}) were inoculated both on b-PPs (negative control) and hep*-NH_2−O_2−PPs and then covered with an acetate film to limit evaporation of the medium. All PPs were incubated with each bacteria strain for 24, 48, and 72 h at 37 °C (≈15% humidity). At the end of each incubation period, PPs were detached from the acetate film, placed in a fresh well containing PBS (pH:7.4), and gently washed to remove unbound cells. The concentration of live bacteria in this washing solution was analyzed after culturing in tryptic soy agar (TSA) plates. In addition to this analysis, the rinsed PPs were also transferred to the tubes containing 1 mL of fresh TSB medium and

vortexed for about 1 min to detach all the remaining bacteria on the surface of the PPs before the PPs were removed. The remaining TSB suspensions consisting of bacteria were diluted ($1/10^2$, $1/10^4$, and $1/10^6$) by fresh TSB addition and cultured at 37 °C for 24 h in TSA plates, respectively. This approach aimed to examine the surface behavior, which can either kill the bacteria upon contact (contact-killing) or limit them from diffusing through the material (bacteria-repellent).[46] Ultimately, bacteria viability was analyzed by counting the number of colonies formed in the agar plates.

2.8. Hemocompatibility Testing

In clinical practice, the typical hemocompatibility of implanted materials is evaluated by testing the interaction between blood-contacting biomaterials with blood and blood components, particularly under kinetic conditions.[7] To assess the anticoagulation behavior (hemolysis) and kinetics (kinetic-blood coagulation test) of the developed PPs, whole human blood was treated with calcium chloride ($CaCl_2$) following a previous method.[47] Next, the bare and heparinized PPs were placed into a 24-well plate, subjected to 100 µL of $CaCl_2$-activated whole blood, and incubated at 25 °C for 1 h. The UV–vis spectrum of free hemoglobin (Hb), encapsulated by erythrocyte, has a characteristic absorbance at 540 nm. Therefore, the kinetic data were obtained from spectrophotometric scanning of the aliquots collected at the predetermined time points (10, 20, 40, and 60 min) as the measured intensities were directly proportional to the Hb concentration.

Additionally, hemolysis testing was conducted to evaluate the kinetic blood coagulation at the blood-material interface. This procedure measures the absorbance of unbound Hb (Equation (1)), which corresponds to non-coagulated blood. In other words, high absorbance values indicate a high amount of free Hb exists, pointing out lower coagulation.[5,22,48] The hemolysis ratio of each solution was obtained from the following equation: The A_s represents the sample's absorbance, A_{nc} is the absorbance of diluted blood with PBS and, A_{pc} corresponds to the diluted blood with DI water as negative and positive control groups, respectively.

$$\%\ \text{Hemolysis Ratio} = \left[\frac{A_s - A_{nc}}{A_{pc} - A_{nc}}\right] \times 100 \quad (1)$$

This study is approved by TOBB-ETU Clinical Research (KAEK-118/122/18.05.2022).

2.9. Platelet Adhesion Testing

The amino acid sequences of the adsorbed proteins can activate surface receptors of the platelets, hence initiating the formation of the aggregates, coagulation, and fibrin formation.[2,39] This mechanism determines the lifetime of the blood-contacting biomaterials, accordingly, examined in this study.

Before platelet adhesion testing, fresh human blood samples were first centrifuged at 1000 × *g* for 15 min to separate platelet-rich plasma (PRP) from the blood. After that, the PPs were placed in a 24-well plate, and 1 mL of PRP was introduced onto the substrate surfaces and incubated for 2 h at 37 °C. Next, the PRP introduced PPs were washed with UPW, and the substrates were treated with 2.5% glutaraldehyde (GA) at 4 °C for 30 min to fix the platelets adhered to the PPs' surface. Finally, the samples were dehydrated by rinsing in ethanol prepared in various concentrations (ethanol % in UPW, 0%, 25%, 50%, 75%, and 100%) and air-dried.[7] The platelets adhered to the PPs surface were investigated by SEM images (magnifications; ×150, ×500; ×2500; ×5000; ×50 000 accelerating voltage and spot size were adjusted to 5–10 kV and 2.0 µm).

This study is approved by TOBB-ETU Clinical Research (KAEK-118/122/18.05.2022).

2.10. Cell Viability

In vitro cytocompatibility of free-heparin, b-PPs, and plasma-modified PPs were performed by the MTT assay tested against BJ healthy human skin fibroblast (ATCC, CRL-2522) cell line following a standard protocol. Briefly, the BJ cells were cultured using MEM supplemented with 10% FBS, 1% sodium pyruvate solution, 1% L-glutamine, and 1% penicillin-streptomycin. Fibroblasts were incubated (Thermo Fisher Scientific, Waltham, MA, USA) at 37 °C in a humidified 5% CO_2 atmosphere. The cells were dissociated with 0.25% trypsin-0.05% EDTA solution, centrifuged and resuspended in a complete medium before cell seeding. Within this scope, 10^4 BJ cells $well^{-1}$ were seeded and incubated for 24 h to obtain a monolayer culture. Following medium aspiration and DPBS washing to remove dead/unbound cells, free-heparin (300 or 400 µg), b-PP surfaces, and plasma-modified hep*-NH_2—O_2—PPs were transferred to the wells and incubated with MEM medium for 24 h. The heparin-free MEM and b-PPs were used as a negative control for free-heparin and plasma-modified PPs, respectively. At the end of 24 h, the mediums were removed, and cells were washed gently with DPBS to remove dead or unbound cells. After subsequent washing, an FBS-free medium containing 0.5 mg mL^{-1} of MTT was added to each well. Following 4 h of incubation, mediums were gently aspirated and washed with DPBS. For evaluating the cell viability, formazan crystals were dissolved in DMSO, and optical densities were spectrophotometrically measured with a microplate reader (Thermo Scientific, Multiskan GO Microplate Photometer) at 540 nm.

3. Results and Discussion

3.1. Optimization of Plasma Processing Parameters

Polypropylene, which has been extensively used as a blood-contacting material, was dual-functionalized by a plasma-enhanced modification strategy for increased hemocompatibility and antibacterial properties. To achieve this, a two-step plasma modification strategy was followed. First, the bare PP surfaces were etched by O_2 glow discharge to create negatively charged[49] hydrophilic and rough surfaces with higher surface area. Following that, an amine-rich film layer was formed in an EDA:NH_3 precursors-generated plasma environment

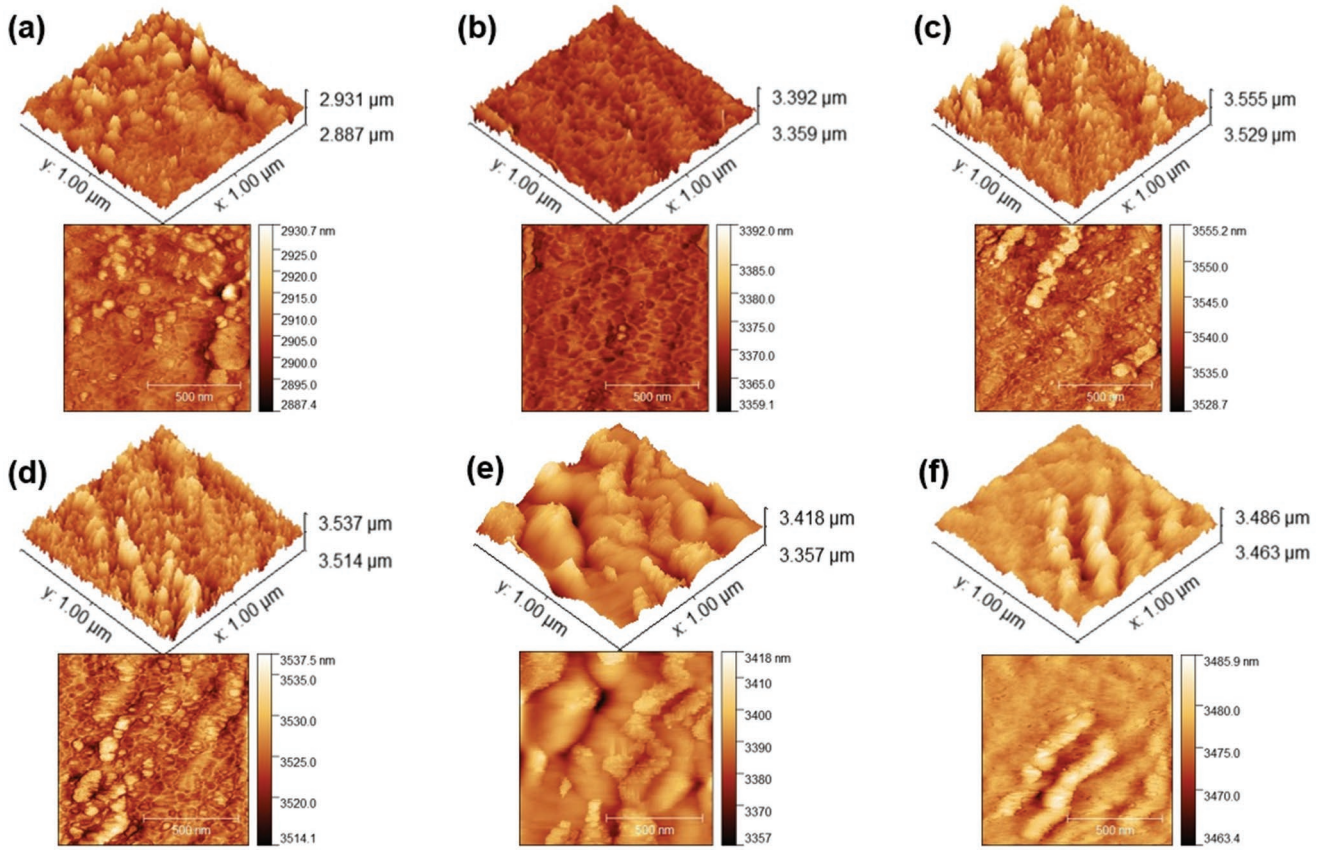

Figure 2. 3D AFM micrographs of the a) unmodified (b-PP), b) oxygen-etched PPs (O_2—PP), and amine-rich film-modified NH_2—O_2—PPs under discharge powers of c) 25 W, d) 50 W, e) 75 W, and f) 100 W.

(25–100 W for 15 min). Throughout the optimization process, detailed surface analyses of the modified PPs were carried out by CA measurements, AFM, XPS, and ATR-FTIR analyses.

The AFM images (**Figure 2**) indicated that, after exposing b-PPs to an O_2 glow discharge, the surface roughness of the b-PPs was slightly raised from 2.45 nm ± 0.80 to 5.81 nm ±1.92. Following plasma polymerization using EDA:NH_3 precursor at 25 and 50 W discharge powers, the O_2—PPs surface became smoother (1.97 nm ± 0.59 and 2.83 nm ± 0.69 for 25 and 50 W, respectively) compared with the O_2—PPs, pointing out the accumulation of the amino-rich film within the protrusions and valleys of the O_2—PPs film matrices. By increasing the power from 75 to 100 W, the Rq of NH_2—O_2—PPs declined significantly to 1.52 nm ± 0.71, much lower than both O_2—PPs (Rq = 5.81 nm ±1.92) as well as, 75 W-treated NH_2—O_2—PPs (Rq = 5.84 nm ±1.92). This reduction in surface roughness is plausibly due to the formation of C-rich (Table S1, Supporting Information, see below for more discussion) bulky film on the substrate that smoothens the surface of the PP-based biomaterial. Therefore, the NH_2—O_2—PPs produced with 75 W 15 min plasma processing parameters were selected as optimal.

XPS analyses were conducted to identify the chemical composition of plasma-modified PPs. After spectral data evaluation and deconvolution, binding energies corresponding to specific bonds were found using tabulated values (**Figure 3**). The significant contribution of C 1s (Figure 3a) core-level spectra at around 285.0 eV was attributed to C—C and C—H single bonding.[50] On the other hand, a single C—O bond at 286.4 eV arose from the O_2 pretreatment on the PP substrate, although the amino group-containing film coating lowered its intensity. The N 1s (Figure 3b) peak having 400.5 eV binding energy corresponds to the C—NH peak, and also the accompanying contribution of the overlapped peaks (401.4 and 402.8 eV) implies the existence of protonated primary amine groups (NH_3^+),[51] suggesting that the amine-rich film polymerization step was effective.

Additionally, the elemental contribution of each plasma-modified film was evaluated (Table S1, Supporting Information). A reduction in the carbon content, especially for NH_2—O_2—PPs produced with 75 W plasma power, is expected to arise from the deposited amino-containing film onto the C-rich polymeric substrate. Also, the highest amino group formation was achieved at that power level, as confirmed by its highest nitrogen content (3.71%). However, the nitrogen percent decreased when the power was elevated to 100 W. This result implies that lower discharge powers than 100 W were adequate to deposit a higher number of amino groups on the O_2-b-PPs surface,[52,53] and increasing the power to 100 W disturbed the amine group formation, which can be related to the shielding effect. Due to increased plasma power, the EDA molecule tends to dissociate from C-based bonds and deposit C-rich bulky films shielding the protrusion of NH_2 groups on the biomaterial surfaces as

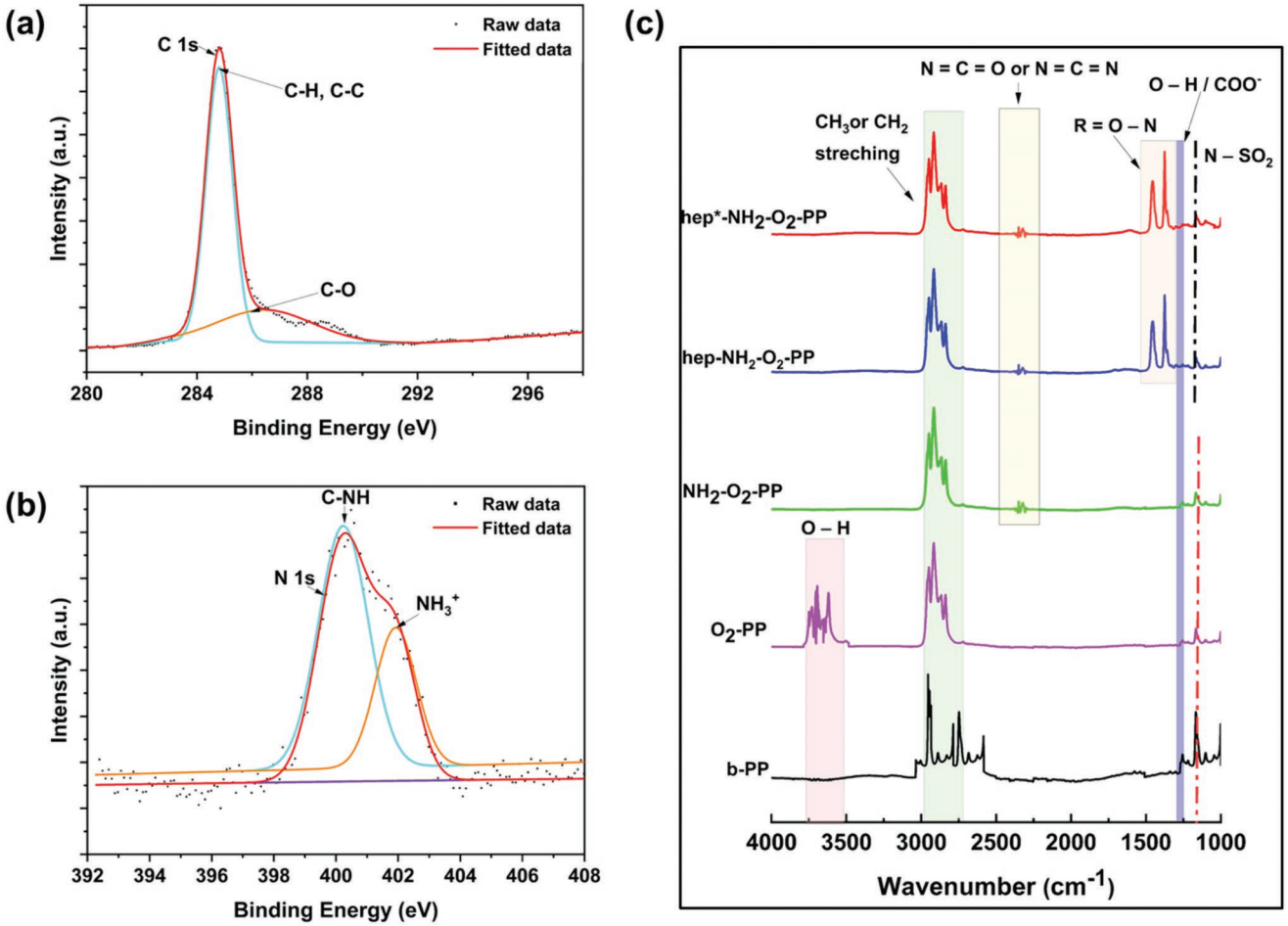

Figure 3. XPS spectra of $-NH_2-O_2-$PPs, a) C 1s, and b) N 1s spectra of NH_2-O_2-PPs modified under 75 W plasma power for 15 min of exposure time. c) FTIR spectra of plasma (un)modified and heparinized PPs.

reported by us and others.[52,54] A comparable amount of O content for the NH_2-O_2-PPs produced by 50 and 75 W plasma power can probably be linked to the post oxidation of a similar number of amino groups deposited.[55,56] All in all, 75 W plasma power was decided as optimum and used for amino-group containing film modification on the PPs' surface.

3.2. Heparin Immobilization and Stability Testing

Heparin is a type of glycosaminoglycan with a molecular weight of 15–20 kDa (120–180 USP units mg^{-1}) and has varying sizes between 1.6 and 2.24 nm. It consists of multiple functional groups (e.g., amino, carboxylic acid, sulfate, and hydroxyl groups) within its structure and also exhibits the highest net negative surface charge (≈−50 mV) among biomolecules.[57,58]

Heparinizing the surface of implant materials is an extensively applied method to avoid blood clotting, sepsis, and/or infection.[4,40] Therefore, in clinical routine, biomaterials are subject to heparinization by directly dipping into a heparin-containing solution before being implanted prior to usage. Once the biomaterial is implanted, repeated dosages (routinely three times a day, 20–40 mg dosage^{-1}) of heparin must be intravenously administered due to the non-specific adsorption and the low stability of heparin on the polymeric material surface. However, this requirement results in overdosage heparin administration and several complications (e.g., thrombocytopenia[59] and abnormal bleeding) may arise that limit the safe and long-term use of the biomaterial. To overcome these limitations, we followed a plasma-enhanced modification strategy to tailor the surface-related features of a common implantable material, polypropylene, for efficient heparin immobilization. Heparin immobilization onto surface modified PPs was carried out following either electrostatic interaction or chemical cross-linking. The effectiveness of each immobilization approach was compared in terms of heparin immobilization capacity and stability.

Toluidine Blue (TB) can irreversibly bind to polyanionic components, such as heparin, and forms a biocomplex. TB has a fingerprint in the UV–vis region at 630 nm; after creating a biocomplex with heparin or heparin-consisting material, its regular intensity decreases at the same wavelength, and that reduction can be used to calculate the amount of the immobilized heparin.[26] In this study, the same strategy was followed to determine the surface density of the immobilized heparin after introducing three different heparin concentrations (3, 10, and 30 mg mL^{-1}) onto the NH_2-O_2-PPs (75 W-15 min) through

Table 1. The contact angle analyses result for unmodified (b-PP) and modified (O—-PPs, NH_2—O_2—PPs, hep/hep*-NH_2—O_2—PPs samples.

Sample	Wettability [°]	Dispersive component [mJ m^{-2}]	Polar component [mJ m^{-2}]	Total SFE [mJ m^{-2}]
b-PP	79.35 ± 6.06	31.89	4.73	36.62
O_2—PP	6.50 ± 0.67	49.04	31.23	80.27
NH_2—O_2—PP	34.72 ± 5.92	38.53	27.38	65.91
hep—NH_2—O_2—PP	40.58 ± 2.89	41.65	14.36	56.01
hep*-NH_2—O_2—PP	32.95 ± 2.07	39.13	11.21	50.34

electrostatic interaction (b-PP, and hep-NH_2—O_2—PPs) as well as covalent bonding (b-PP and hep*-NH_2—O_2—PPs).

First, the influence of electrostatic interaction formed between amino-containing films and heparin was evaluated by TB screening. The adsorbed heparin amounts calculated were as follows: 207.19 ± 34.33 μg cm^{-2}, 61.48 ± 8.03; 28.17 ± 5.77 μg cm^{-2} for 30 mg mL^{-1}, 10 mg mL^{-1}, 3 mg mL^{-1}, respectively. Due to the highest heparin adsorption achieved at 30 mg mL^{-1} heparin concentration, this concentration was used for the covalent coupling. The results indicated that when 1:1 (w:w). heparin:(EDC/NHS) was used to couple 30 mg mL^{-1} of heparin onto the surface of NH_2—O_2—PPs, and the immobilized heparin concentration was raised to 440.41 ± 69.52 μg cm^{-2} (≈27 mg considering the total material surface area), which is significantly higher compared to the one-time applied dosage range administered in the clinic (≈20–40 mg). Moreover, as predicted, the covalent binding suggested a much better heparin immobilization performance than the electrostatically coupled material (hep—NH_2—O_2—PPs).

The stability results were carried out by dipping hep*-NH_2—O_2—PPs into a PBS (pH:7.4) buffer and screening aliquots drawn at the predetermined time points over 30 days. Although the hep*-NH_2—O_2—PPs released almost 90% of heparin within the first day, the remaining immobilized heparin amount remained constant throughout 29 days at 28.99 ± 3.17 μg cm^{-2}, which is much lower than the toxic dose indicated in the literature.[59]

3.3. Physicochemical Characterization of Heparin-Modified Materials

Further analyses were carried out to evaluate the resultant biomaterial and see the influence of each modification step. ATR-FTIR analysis (Figure 3c) revealed significant changes in the surface chemistry of the b-PPs. Polypropylene has a fingerprint at around 2700–2900 cm^{-1}, corresponding to symmetric and asymmetric stretching of CH_3 and CH_2 groups.[12] Upon O_2 etching, O—H stretching vibrations appeared on the IR spectra between the 3550–3700 cm^{-1} range.[60] Amine-rich plasma polymerization resulted in primary amine groups (N = C = O, N = C = N) formed at about 2300 cm^{-1}, confirming the amine-layer formation onto O_2—PPs.[12] Followingly, heparin existence was proved for hep—NH_2—O_2—PPs, and hep*-NH_2—O_2—PPs by the increased sulfur content revealed around 1350 and 1370 cm^{-1}, corresponding to asymmetric SO_2 and/or N—SO_2 vibration of heparin.[50] The difference between hep—NH_2—O_2—PPs and hep*-NH_2—O_2—PPs spectra was three peaks. The first peak observed at about 1301–1252 cm^{-1} related to —OH and/or C—O carboxylic acid groups,[61] the second one seen at 1168 cm^{-1} exhibiting the C—O stretching or N-sulphation groups,[62,63] and most importantly amide II and III peak from beginning 1400–1500 cm^{-1} and, 1250–1350 cm^{-1}, respectively, confirming covalent linkage.[64]

Static contact angle measurement via a sessile drop technique is an extensively applied approach that evaluates the wetting characteristics and SFEs; particular interest is given to the plasma-modified thin films. Therefore, the surface wettability and SFE of the native substrates, plasma-treated PPs, and heparinized surfaces (**Table 1**) were examined. The b-PP surfaces exhibited a hydrophobic (79.35° ± 6.06°) nature due to the dominance of C—H/C—C groups within the polymer matrice. Upon O_2 treatment, the b-PP surfaces became superhydrophilic (6.50° ± 0.67°), and the disruption of intermolecular bonds of PPs by added polar functional groups (e.g., C—O, C = O) increased the SFE of the b-PPs from 36.62 to 80.27 mJ m^{-2}. However, a significant change in wettability was observed upon amine functionalization. The amine-rich film formation induced the active surface area (where the immobilization will occur) of the PPs while retaining its hydrophilicity (34.72° ± 5.92°). In addition, due to impinging plasma particles breaking C—C/C—H bonds in the PP-substrate, highly energetic free radicals (65.91 mJ m^{-2}) were formed that plausibly facilitate the immobilization of heparin.[65,66] Subsequently, the contact angle values were decreased upon heparin incorporation proportionally with the amount of immobilized heparin on the NH_2—O_2—PP substrates. The contact angle of surface adsorbed hep—NH_2—O_2—PP substrates was 40.58° ± 2.89° (56.01 mJ m^{-2}), and hep*-NH_2—O_2—PPs were 32.95° ± 2.07° (50.34 mJ m^{-2}), both found much more hydrophilic compared with the unmodified b-PPs. The higher hydrophilicity of the hep*-NH_2—O_2—PPs can be attributed to the incorporation of highly polar C—O, C=O, C—H, and O—C = O groups present on the surface of substrates. The increased hydrophilicity of the hep*-NH_2—O_2—PPs can be attributed to the incorporation higher number of polar and charged —COOH and SO_3^- groups for the covalently-modified surface. Due to such prospects, the hep*-modified samples were utilized in the remaining part of this report along with the control groups.

3.4. Protein Adsorption

Protein adsorption to biomaterials' surfaces significantly depends on the surface characteristics of the biomaterial, such as hydrophilicity, roughness, and surface charge. In the

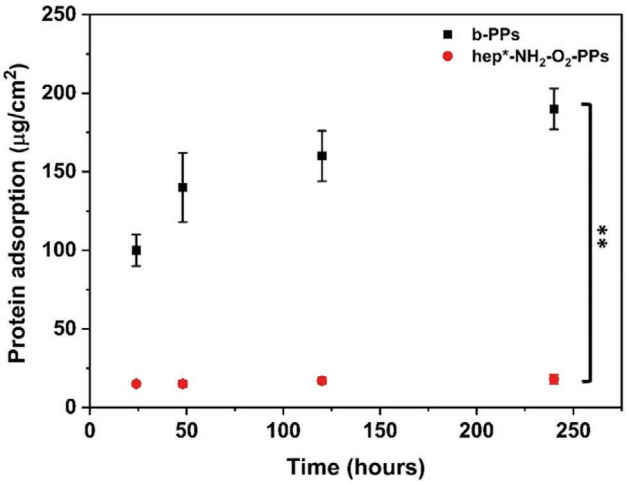

Figure 4. BSA protein adsorption testing of the unmodified and heparinized PPs ($n = 9$, (**$p > 0.005$)).

literature, it has been shown that albumin and fibrinogen had no binding affinity to heparin at physiological pH.[5,24] In line with these reports, we have conducted the adsorption analysis of albumin on the heparin-modified substrates and native PPs. **Figure 4** shows that the unmodified b-PPs had BSA adsorption levels of 190 ± 13 μg cm^{-2}, which drastically decreased to 13 ± 3 μg cm^{-2} for hep*-NH_2—O_2—PPs. The isoelectronic point of BSA is 4.8, and at physiological pH, it has a net negative charge. Since heparin is also highly negative at this pH due to carboxylic acid and sulfonate groups, BSA adsorption is significantly suppressed on the covalently modified surface compared to the unmodified counterpart.[19–21]

3.5. Antibacterial Activity

Bacterial infections caused by the implanted materials can cause several problems by exhibiting complex adhesion mechanisms depending on the strain type, resulting in drug resistance, implant failure, and even patient mortality.[6] For instance, implant devices cause approximately 45% of all nosocomial infections that are highly resistant to antibiotics and host defenses and frequently persevere until the infected implanted material is removed.[67] Therefore, evaluating the interaction between a specific biomaterial and different bacteria strains is essential for ensuring its safe usage in clinics.

The antibacterial characteristics of b-PP and hep*-NH_2—O_2—PP substrates against *S. epidermidis*, *S. aureus*, and *E. coli* were tested.[68] Each bacterium colony was quantitatively studied in terms of a colony forming unit (CFU) per volume (CFU mL^{-1}). Before assay examination, the reproduction of the bacteria was controlled, and TSA was taken as a negative control to evaluate the possible contaminations and bacterial growth.

S. epidermidis is a gram-positive and coagulase-negative bacterium that belongs to the *Staphylococcus* species. When a specific implant causes nosocomial infection, this bacterium enters a patient's bloodstream, causing several unwanted interactions, such as sepsis, if not diagnosed and treated early.[67,69] Because of these reasons, antibacterial studies were first carried out against *S. epidermidis*. **Figure 5**a shows that *S. epidermidis* is present extensively in the vicinity of the bare PP substrates as they can colonize if the washing solution of this substrate is utilized. Moreover, significant colony formation was observed when the adsorbed bacteria on this substrate were removed and cultivated (Figure 5b). As expected, the number of colonies increased with incubation time in both cases. On the contrary, when the hep*-NH_2—O_2—PP substrates were employed, the washing solution and the detached-pathogen-containing medium did not cause significant colonization. Increased incubation times with the substrates further lowered the numbers to negligible levels for both bacterial sources. Similar tendencies were observed when the bacteria type was altered to another gram-positive pathogen, *S. aureus*, or a gram-negative strain, *E. coli*.

In order to elucidate this observed trend, both substrates that were incubated with the three strains for 24 h were rinsed,

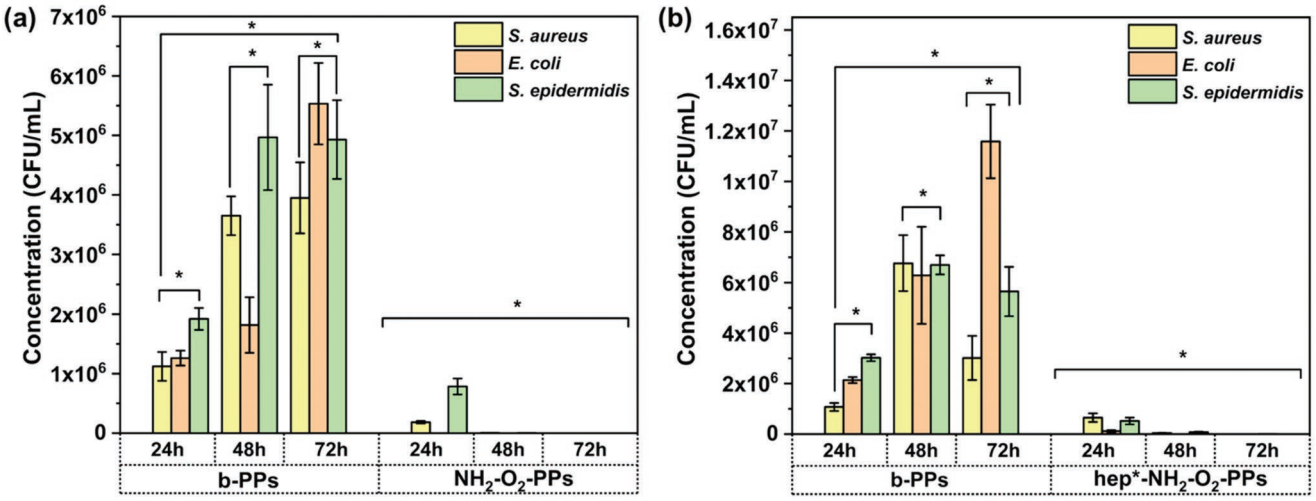

Figure 5. Bacteria colonization of *S. epidermidis*, *S. aureus*, and *E. coli*. a) Bacterial colonies that were not adhered on the b-PPs and heparinized PPs surfaces when immersed in a wash buffer (PBS). b) Bacterial colonies adhered to the b-PPs and heparinized PPs surfaces. Bacteria strains were cultivated on TSA plates, and each bacteria strain was incubated with the substrate of interest for 24, 48, and 72 h at 37 °C ($n = 12$, *$p < 0.05$).

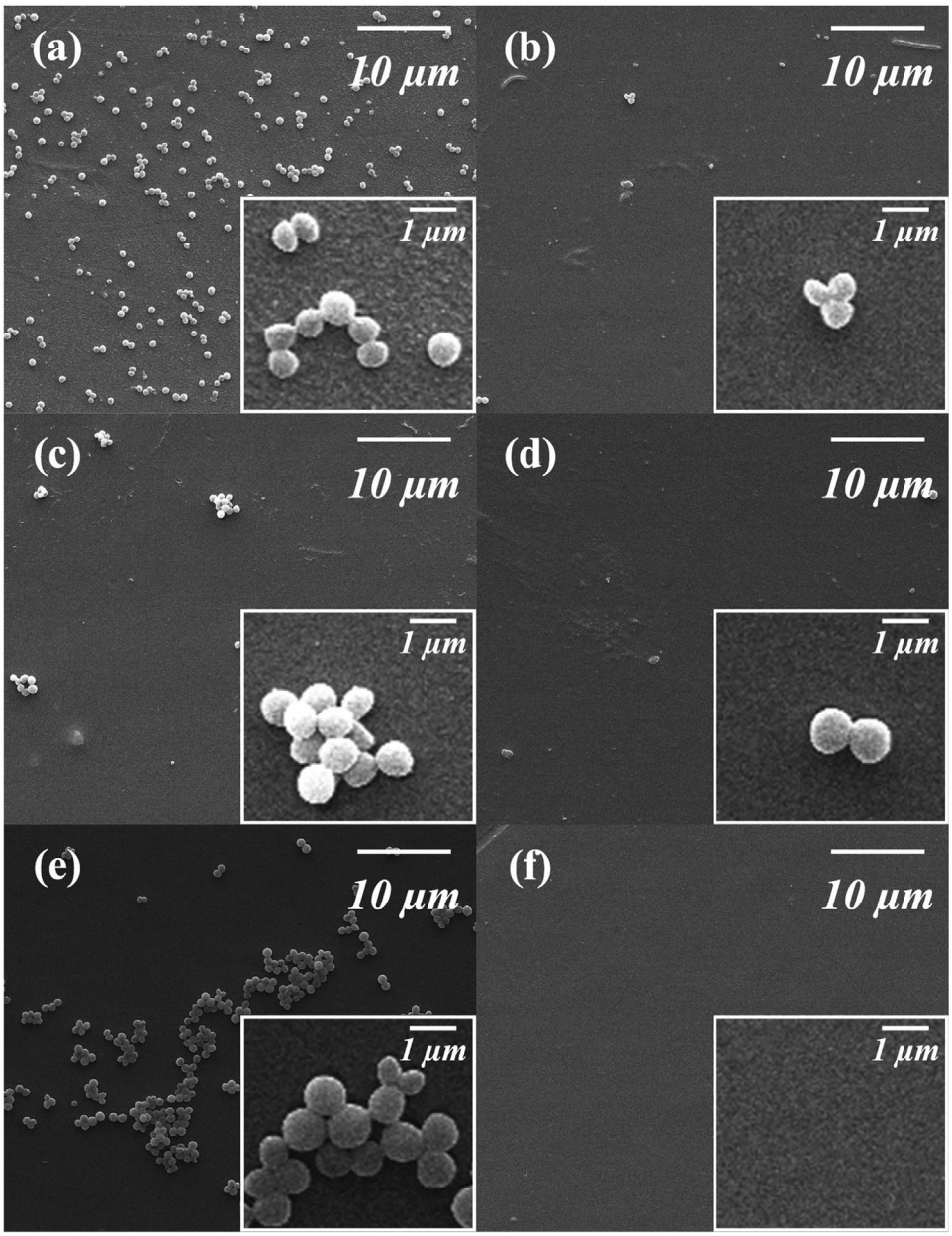

Figure 6. SEM images representing bacteria colonization formed on the unmodified b-PPs and plasma-modified and heparinized PPs (hep*-NH_2—O_2—PPs) against gram-positive *S. aureus* and *S. epidermidis* and gram-negative *E. coli* after incubated for 24 h. The SEM images were taken following 24 h of incubation of each strain with the plasma (un)modified PPs. *S. aureus* incubated with a) b-PPs and b) hep*-NH_2—O_2—PPs. *E. coli* incubated with c) b-PPs and d) hep*-NH_2—O_2—PPs. *S. epidermidis* incubated with e) b-PPs and f) hep*-NH_2—O_2—PPs. All images were taken at the magnification of ×5000 and ×50 000.

and surface electron micrographs were taken. **Figure 6** clearly shows that the b-PP surfaces promote bacterial adhesion for all strains, whereas the heparin-modified counterpart's surfaces are highly anti-adherent. Such micrographs evidently explain the extremely poor colonization of vortexed samples in Figure 5b. Here, the colonized bacteria concentration at the end of 24 h is almost wholly diminished for 48 and 72 h durations. The reduction in colonization in extended periods can have two components: contact-killing and released-heparin influence. We suspect that these factors, which are not present in b-PP samples, are also the main reasons for the absence of bacterial species in the washing solutions of heparin-modified substrates, as displayed in Figure 5a. For the latter samples, heparin modification brought higher polarity and negative charge by the sulfate groups, which could easily interact or/and chelate with the cations that play a crucial role in bacterial growth, or heparin modification might have disturbed the stable hydrogen bonding in the bacteria environment otherwise via direct binding to the bacteria and caused their death.[55,70,71] Extend durations here also provide higher chances of contact-killing

and effective removal of even highly resistant bacteria from the washing solutions, yielding >99% antibacterial characteristics compared to bare-PP counterpart. The reduced viabilities may also be caused by the released heparin, which was quantified to be 410 μg cm^{-2} after 24 h. Although this amount is below the MBC levels shown in Figure S1, Supporting Information, much lower bacterial loadings were employed on the PP substrates. A simple ratiometric calculation reveals that the released amount corresponds to heparin concentrations over MBC levels. It is crucial to note that, in the following sections, the same released heparin concentrations were found as non-cytotoxic when fibroblasts were employed at similar cellular densities (≈10^4 cells $well^{-1}$).

3.6. Hemocompatibility Testing

Hemolysis can be defined as the distortion of the membrane structure of the red blood cell, causing the release of hemoglobin into the plasma. Following such an approach, the interaction between red blood cells with b-PP and hep*-NH_2—O_2—PPs was evaluated (n = 6). Within the hemocompatibility tests, blood samples drawn from four different healthy volunteers were exposed to the two PP substrates for 1 h. Hemolysis ratios were calculated as 2.18 ± 0.04% and 0.45 ± 0.02% for the b-PP and hep*-NH_2—O_2—PPs, respectively, fulfilling the ISO-10993-5 criteria (Hemolysis ratio (%) < 5%).[72] The hemolysis ratio of erythrocytes exposed to TCPS controls (blank well) was used as a reference.

A similar approach was applied for the kinetic blood coagulation tests; the only difference is that the screening was conducted at different time points for up to an hour to examine the coagulation kinetics of the blood when interacted with the b-PPs, hep*-NH_2—O_2—PPs, and TCPS control (n = 6, **Figure 7**). After the incubation period, blood samples remaining uncoagulated were exposed to UPW and released free hemoglobin subjected to spectral measurements. Thus, the absorbance readings in the UV–vis spectra are proportionally linked with the amount of free hemoglobin. The remaining hemoglobin joins to the clot formation resulting in coagulation; hence, higher absorbance values indicate better hemocompatibility results. The absorbance readings implied an insufficient difference (p > 0.05) between the blood coagulation behavior of b-PP and hep*-NH_2—O_2—PP substrates within the first 40 min of incubation, although the heparin conjugation consistently caused higher free hemoglobin levels. However, after 60 min of treatment, hep*-NH_2—O_2—PPs surfaces displayed a discrete difference compared to unmodified counterparts and the TCPS controls, reaching fivefold–tenfold higher absorbance values indicating much lower risks of blood coagulation.

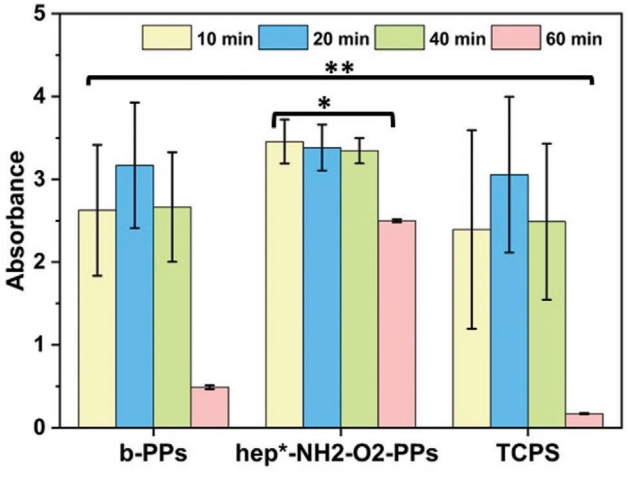

Figure 7. Kinetic-blood coagulation testing results of the b-PPs, plasma-modified PPs (hep*-NH_2—O_2—PPs), and TCPS controls (n = 6, *p < 0.05, **p < 0.01).

3.7. Platelet Adhesion Test

The aggregation of platelets triggers thrombus formation at the biomaterial-blood interface that may cause potential risks to the patient, especially when implanted in vivo. Therefore, in addition to hemocompatibility analysis, it is vital to investigate platelet adhesion and activation features on the implant surfaces. Platelet adhesion studies were conducted by testing the blood samples drawn from four healthy volunteers. The blood samples were first centrifuged, and the plasma consisting of PRP (1 mL) was incubated with the b-PPs and hep*-NH_2—O_2—PPs (n = 3) to analyze the interaction between platelets and the PPs surfaces. It can be inferred from **Figure 8** that unmodified b-PPs stimulated platelet adhesion and accumulation. On the contrary, for hep*-NH_2—O_2—PPs, platelet adhesion was drastically reduced due to the incorporation of reactive functional groups on the immobilized heparin, including carboxyl and sulfonate moieties that effectively repel the interacting platelets.[73]

3.8. In Vitro Cell Viability

PP is a heavily used polymeric material in clinics, and it was expected for this material to fulfill the non-cytotoxicity standard of ISO 10993–5.[72] As the implanted material will be in contact with a physiological environment, it has to fulfill several quality standards, including biocompatibility and safety,[74] before being approved by the health authorities for patient use. Therefore, to evaluate the biocompatibility of the plasma-modified PPs, their cytotoxicity against BJ cells was tested. The cells were incubated with different concentrations of free-heparin, hep*-NH_2—O_2—PPs, and b-PPs for 24 h. The in vitro cytotoxicity results imply that compared to the TCPS control (100.17 ± 3.14%), both b-PPs and hep*-NH_2—O_2—PPs enhance cellular viabilities, yielding 111.85 ± 8.65% (p > 0.05 vs TCPS) and 141.16 ± 6.82% (*p < 0.05 concerning b-PPs), respectively (**Figure 9**). The plasma-assisted heparin conjugation improved fibroblast viabilities compared to the native PP biomaterial.

The final part of this report investigated potential cytotoxicity induced by the released free heparin from the hep*-NH_2—O_2—PPs. Two different concentrations, 300 and 400 μg of heparin were selected considering the released amount of free heparin from hep*-NH_2—O_2—PPs substrates in section 3.2 (≈330.04 ± 70.56 μg). After free heparins were incubated with

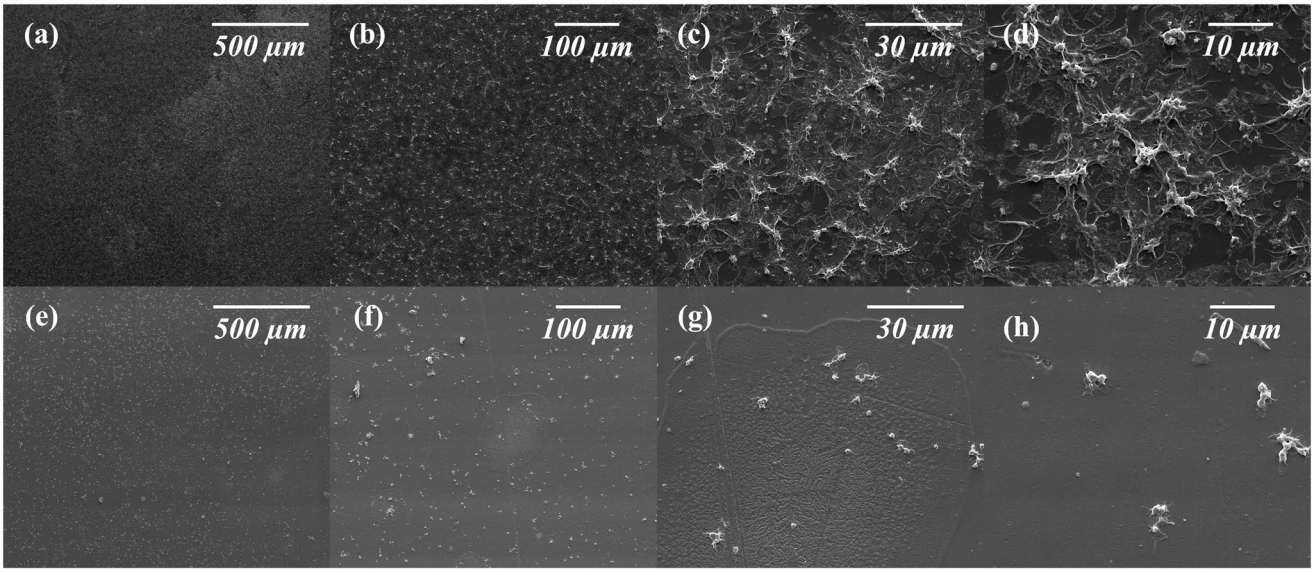

Figure 8. SEM images of a–d) b-PPs and e–h) hep*-NH_2—O_2—PPs that were incubated with PRP extracted from human blood. The SEM images were taken at a,e) ×150, b,f) ×500, c,g) ×2500, d,h) ×5000 of magnifications.

the BJ cells, 119.65 ± 7.43% and 111.79 ± 5.52% cell viability were recorded, respectively (*$p < 0.05$ concerning TCPS). Such results confirm that the surface-tailored hep*-NH_2—O_2—PPs are not only a non-toxic material but can also enhance cellular viability much more than a previously published work.[22,75]

4. Conclusions

In summary, the surface of PPs has been activated by oxygen plasma etching that later functionalized with amine-rich plasma treatment before subsequent covalent heparin immobilization. The oxygen pretreatment resulted in a rougher surface compared to the native PPs; meanwhile, its surface area was enhanced with anionic —OH groups. In addition, subsequent plasma functionalization with the EDA:NH_3 precursor mixture (at 75 W power for 15 min exposure time) resulted in the incorporation of highly hydrophilic (34.72° ± 5.92°) and energetic (65.91 mJ m^{-2}) cationic primary amine groups (N = C = O, N = C = N), confirming the amine-layer formation onto the pre-treated PPs' surfaces. These modifications later facilitated sufficient heparin loading (≈440 μg cm^{-2}) by a covalent linkage confirmed by the amide peak shown in the ATR-FTIR spectra.

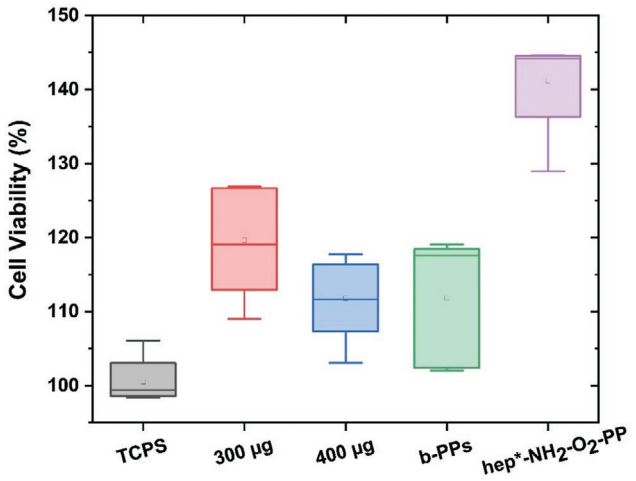

Figure 9. MTT cytotoxicity results of BJ cells treated with 300 and 400 μg of free-heparin and hep*-NH_2—O_2—PPs compared to TCPS and b-PPs controls, respectively ($n = 5$, *$p < 0.05$).

In the meantime, hemocompatibility studies were evaluated to investigate the biomaterial's kinetic blood-clotting, hemolysis, protein, and platelet adhesion features. The hemocompatibility analyses showed that the heparinized PPs surfaces lowered the hemolysis ratio and protein adsorption about fivefold–tenfold and 15-folds concerning the unmodified PPs. Meanwhile, platelet adhesion was considerably dropped on the heparinized PPs surfaces due to repelling of carboxyl and sulfonate moieties. Besides, heparin immobilization provided an anti-adhesive and antibacterial film layer that reduced the bacterial adhesion, particularly by contact-killing gram-negative and -positive bacteria strains up to 99%, as desired from a robust antibacterial coating that restricts any possible infection once contacted with blood. More importantly, although the remaining heparin content after 24 h considerably lowered to 30 μg cm^{-2}, the remaining portion still presented a hydrophilic surface with highly suppressed protein adsorption and platelet adhesion characteristics but, simultaneously, improved antibacterial properties.

Considering the previously published works,[13,15,19,25,29,30,50] our facile heparin conjugation approach can render the conventional PPs a safer biomaterial with better antibacterial and hemocompatibility performance. Ultimately, the offered alternative implant modification scheme can become a universally applied strategy where coagulation-related complexities are of prime interest during and post-implantation of upcoming blood-contacting materials.

Supporting Information

Supporting Information is available from the Wiley Online Library or from the author.

Conflict of Interest

The authors declare no conflict of interest.

Data Availability Statement

The data that support the findings of this study are available from the corresponding author upon reasonable request.

Keywords

biofilm formation, clot formation, hemocompatibility, platelet adhesion, protein adhesion

Received: September 9, 2022
Revised: October 25, 2022
Published online:

[1] J. M. Courtney, N. M. K. Lamba, S. Sundaram, C. D. Forbes, *Biomaterials* **1994**, *15*, 737.
[2] M. B. Gorbet, M. V. Sefton, *Biomaterials* **2004**, *25*, 5681.
[3] R. Sabino, K. Popat, *Bio-Protoc.* **2020**, *10*, e3505.
[4] X. Zhao, J. M. Courtney, *Surf. Modif. Biomater.,* **2011**, pp. 56–77.
[5] C. Zhao, X. Liu, M. Nomizu, N. Nishi, *Biomaterials* **2003**, *24*, 3747.
[6] W. Ahmed, Z. Zhai, C. Gao, *Mater. Today Bio* **2019**, *2*, 100017.
[7] Y. Jin, Z. Zhu, L. Liang, K. Lan, Q. Zheng, Y. Wang, Y. Guo, K. Zhu, R. Mehmood, B. Wang, *Appl. Surf. Sci.* **2020**, *528*, 146539.
[8] S. Taheri, A. Cavallaro, S. N. Christo, L. E. Smith, P. Majewski, M. Barton, J. D. Hayball, K. Vasilev, *Biomaterials* **2014**, *35*, 4601.
[9] F. Kara, E. A. Aksoy, Z. Yuksekdag, S. Aksoy, N. Hasirci, *Appl. Surf. Sci.* **2015**, *357*, 1692.
[10] E. Evren, E. Yurtcu, *Folia Microbiol.* **2015**, *60*, 351.
[11] A. Gopanna, K. P. Rajan, S. P. Thomas, M. Chavali, *Mater. Biomed. Eng.: Thermoset Thermoplast. Polym.* **2019**, *8*, 175.
[12] R. Li, H. Wang, W. Wang, Y. Ye, *J. Biomater. Sci., Polym. Ed.* **2013**, *24*, 15.
[13] Y. J. Kim, I. K. Kang, M. W. Huh, S. C. Yoon, *Biomaterials* **2000**, *21*, 121.
[14] C. A. K. Bajpai, S. Kankane, S. K. Singh, *J. Dispersion Sci. Technol.* **2011**, *32*, 1032.
[15] J. L. Chen, Q. L. Li, J. Y. Chen, C. Chen, N. Huang, *Appl. Surf. Sci.* **2009**, *255*, 6894.
[16] M. C. Yang, W. C. Lin, *J. Polym. Res.* **2002**, *9*, 201.
[17] W. Zhan, X. Shi, Q. Yu, Z. Lyu, L. Cao, H. Du, Q. Liu, X. Wang, G. Chen, D. Li, J. L. Brash, H. Chen, *Adv. Funct. Mater.* **2015**, *25*, 5206.
[18] H. Gu, X. Chen, Q. Yu, X. Liu, W. Zhan, H. Chen, J. L. Brash, *J. Mater. Chem. B* **2017**, *5*, 604.
[19] S. Degoutin, M. Jimenez, F. Chai, T. Pinalie, S. Bellayer, M. Vandenbossche, C. Neut, N. Blanchemain, B. Martel, *J. Biomed. Mater. Res., Part A* **2014**, *102*, 3846.
[20] Z. Zdanowski, B. Koul, E. Hallberg, C. Schalén, **2012**, *8*, 825.
[21] A. Morozan, F. Nastase, A. Dumitru, C. Nastase, S. Vulpe, M. Filipescu, *Phys. Status Solidi C* **2009**, *6*, 2195.
[22] C. J. Pan, Y. H. Hou, B. B. Zhang, Y. X. Dong, H. Y. Ding, *J. Mater. Chem. B* **2014**, *2*, 892.
[23] Z. Yang, J. Wang, R. Luo, X. Li, S. Chen, H. Sun, N. Huang, *Plasma Processes Polym.* **2011**, *8*, 850.
[24] L. C. Winterton, J. D. Andrade, J. Feijen, S. W. Kim, *J. Colloid Interface Sci.* **1986**, *111*, 314.
[25] R. Biran, D. Pond, *Adv. Drug Delivery Rev.* **2017**, *112*, 12.
[26] X. Ren, L. Xu, J. Xu, P. Zhu, L. Zuo, S. Wei, *J. Biomater. Sci., Polym. Ed.* **2013**, *24*, 1707.
[27] S. Alban, *Handb. Exp. Pharmacol.* **2012**, *207*, 211.
[28] B. Rånby, *J. Adh. Sci. & Technol.* **1995**, *9*, 599.
[29] J. Balart, V. Fombuena, J. M. España, L. Sánchez-Nácher, R. Balart, *Mater. Des.* **2012**, *33*, 1.
[30] H. Zhao, J. Wang, Z. Cao, J. Lei, *J. Appl. Polym. Sci.* **2012**, *124*, E161.
[31] V. Hahn, C. Dikyol, B. Altrock, M. Schmidt, K. Wende, U. K. Ercan, K. D. Weltmann, T. von Woedtke, *Plasma Processes Polym.* **2019**, *16*, 1800164.
[32] G. K. Can, H. F. Özgüzar, G. Kabay, P. Kömürcü, M. Mutlu, *MRS Commun.* **2018**, *8*, 541.
[33] H. F. Özgüzar, G. K. Can, G. Kabay, M. Mutlu, *MRS Commun.* **2019**, *9*, 710.
[34] F. Buyukserin, S. Altuntas, B. Aslim, *RSC Adv.* **2014**, *4*, 23535.
[35] I. K. Kang, O. H. Kwon, Y. M. Lee, Y. K. Sung, *Biomaterials* **1996**, *17*, 841.
[36] J. Panzer, *J. Colloid Interface Sci.* **1973**, *44*, 142.
[37] G. Kaleli-Can, H. F. Özgüzar, M. Mutlu, *Appl. Phys. A: Mater. Sci. Process.* **2022**, *128*, 277.
[38] J. T. Gallagher, *Handb. Exp. Pharmacol.* **2012**, *207*, 347.
[39] X. Liu, L. Yuan, D. Li, Z. Tang, Y. Wang, G. Chen, H. Chen, J. L. Brash, *J. Mater. Chem. B* **2014**, *2*, 5718.
[40] G. D. Christensen, W. A. Simpson, A. L. Bisno, E. H. Beachey, *Infect. Immun.* **1983**, *40*, 407.
[41] J. A. Johnson, T. H. Cogbill, P. J. Strutt, A. L. Gundersen, *Arch. Surg.* **1988**, *123*, 859.
[42] T. Wadström, et al., *Pathogenesis of Wound & Biomaterial-Associated Infections*, Springer Science & Business Media, **2012**.
[43] M. Bocé, M. Tassé, S. Mallet-Ladeira, F. Pillet, C. Da Silva, P. Vicendo, P. G. Lacroix, I. Malfant, M. P. Rols, *Sci. Rep.* **2019**, *9*, 1.
[44] H. F. Özgüzar, A. E. Meydan, J. S. Göçmen, M. Mutlu, *MRS Commun.* **2021**, *11*, 523.
[45] G. Kaleli-Can, H. F. Özgüzar, S. Kahriman, M. Türkal, J. S. Göçmen, E. Yurtçu, M. Mutlu, *Mater. Today Commun.* **2020**, *25*, 101565.
[46] Y. Qing, L. Cheng, R. Li, G. Liu, Y. Zhang, X. Tang, J. Wang, H. Liu, Y. Qin, *Int. J. Nanomed.* **2018**, *13*, 3311.
[47] V. B. Damodaran, V. Leszczak, K. A. Wold, S. M. Lantvit, K. C. Popat, M. M. Reynolds, *RSC Adv.* **2013**, *3*, 24406.
[48] C. C. Chou, Y. Y. Wu, J. W. Lee, C. H. Yeh, J. C. Huang, *Surf. Coat. Technol.* **2013**, *231*, 418.
[49] A. Vesel, I. Junkar, U. Cvelbar, J. Kovac, M. Mozetic, *Surf. Interface Anal.* **2008**, *40*, 1444.
[50] K. N. Pandiyaraj, M. C. R. Kumar, A. A. Kumar, P. V. A. Padmanabhan, R. R. Deshmukh, M. Bah, S. I. Shah, P. G. Su, M. Halleluyah, A. S. Halim, *Appl. Surf. Sci.* **2016**, *370*, 545.
[51] E. S. Permyakova, A. M. Manakhov, P. V. Kiryukhantsev-Korneev, A. N. Sheveyko, K. Y. Gudz, A. M. Kovalskii, J. Polčak, I. Y. Zhitnyak, N. A. Gloushankova, I. A. Dyatlov, S. G. Ignatov, S. Ershov, D. V. Shtansky, *Appl. Surf. Sci.* **2021**, *556*, 149751.
[52] A. Choukourov, H. Biederman, I. Kholodkov, D. Slavinska, M. Trchova, A. Hollander, *J. Appl. Polym. Sci.* **2004**, *92*, 979.
[53] F. Truica-Marasescu, M. R. Wertheimer, *Plasma Processes Polym.* **2008**, *5*, 44.
[54] S. Babaei, P. L. Girard-Lauriault, *Plasma Chem. Plasma Process.* **2016**, *36*, 651.
[55] A. Manakhov, D. Nečas, J. Čechal, D. Pavliňák, M. Eliáš, L. Zajíčková, *Thin Solid Films* **2015**, *581*, 7.

[56] K. S. Siow, L. Britcher, S. Kumar, H. J. Griesser, *Plasma Processes Polym.* **2006**, *3*, 392.
[57] U. Lindahl, M. Kusche-Gullberg, L. Kjellen, *J. Biol. Chem.* **1998**, *273*, 24979.
[58] H. J. Gabius, S. André, H. Kaltner, H. C. Siebert, *Biochim. Biophys. Acta, Gen. Subj.* **2002**, *1572*, 165.
[59] L. A. Linkins, T. E. Warkentin, *Semin. Thromb. Hemostasis* **2011**, *37*, 653.
[60] R. Morent, N. De Geyter, C. Leys, L. Gengembre, E. Payen, *Surf. Interface Anal.* **2008**, *40*, 597.
[61] A. Devlin, L. Mauri, M. Guerrini, E. A. Yates, M. A. Skidmore, *bioRxiv* **2019**, 744532, https://doi.org/10.1101/744532.
[62] F. Cabassi, B. Casu, A. S. Perlin, *Carbohydr. Res.* **1978**, *63*, 1.
[63] T. Yang, A. Hussain, S. Bai, I. A. Khalil, H. Harashima, F. Ahsan, *J. Controlled Release* **2006**, *115*, 289.
[64] R. S. Banegas, C. F. Zornio, A. M. G. De Borges, L. C. Porto, V. Soldi, *Polímeros* **2013**, *23*, 182.
[65] C. M. Chan, T. M. Ko, H. Hiraoka, *Surf. Sci. Rep.* **1996**, *24*, 1.
[66] D. J. Lyman, K. Knutson, B. McNeill, K. Shibatani, *Trans. - Am. Soc. Artif. Intern. Organs* **1975**, *21*, 49.
[67] T. T. Timbrook, J. B. Morton, K. W. Mcconeghy, A. R. Caffrey, E. Mylonakis, K. L. LaPlante, *Clin. Infect. Dis.* **2017**, *307*, 15.
[68] J. S. Association, *Japanese Ind. Stand. 2000 ; JIS Z 2801* **2000**.
[69] B. H. Hamory, J. T. Parisi, *Am. J. Infect. Control* **1987**, *15*, 59.
[70] W. Rosett, G. R. Hodges, *J. Clin. Microbiol.* **1980**, *11*, 30.
[71] S. Chandan, N. George, C. Zappala, R. J. Boots, J. Faoagali, *Critical Care and Resuscitation* **2007**, *9*.
[72] ISO 10993-5:2009 Biological evaluation of medical devices — Part 5: Tests for in vitro cytotoxicity https://www.iso.org/standard/36406.html.
[73] D. J. Lyman, J. L. Brash, S. W. Chaikin, K. G. Klein, M. Carini, *Trans Am Soc Artif Intern Organs.* **1968**, *14*, 5701539.
[74] A. Pisac, N. Wilson, *AMA J. Ethics* **2021**, *23*, E712.
[75] H. Hemeda, J. Kalz, G. Walenda, M. Lohmann, W. Wagner, *Cytotherapy* **2013**, *15*, 1174.